Redox Biology 9 (2016) 167–177

Contents lists available at ScienceDirect

Redox Biology

journal homepage: www.elsevier.com/locate/redox

Research Paper

Absorbance and redox based approaches for measuring free heme and free hemoglobin in biological matrices

Joo-Yeun Oh [g,1], Jennifer Hamm [b,1], Xin Xu [c,f], Kristopher Genschmer [c,f], Ming Zhong [c,i], Jeffrey Lebensburger [b], Marisa B. Marques [a], Jeffrey D. Kerby [d,h], Jean-Francois Pittet [e], Amit Gaggar [c,f,h], Rakesh P. Patel [a,g,*]

[a] Departments of Pathology, University of Alabama at Birmingham, Birmingham, AL 35294, United States
[b] Departments of Pediatrics, University of Alabama at Birmingham, Birmingham, AL 35294, United States
[c] Departments of Medicine, University of Alabama at Birmingham, Birmingham, AL 35294, United States
[d] Departments of Surgery, University of Alabama at Birmingham, Birmingham, AL 35294, United States
[e] Departments of Anesthesiology and Perioperative Medicine, University of Alabama at Birmingham, Birmingham, AL 35294, United States
[f] Program in Protease and Matrix Biology, University of Alabama at Birmingham, Birmingham, AL 35294, United States
[g] Center for Free Radical Biology, University of Alabama at Birmingham, Birmingham, AL 35294, United States
[h] Birmingham VA Medical Center, University of Alabama at Birmingham, Birmingham, AL 35294, United States
[i] Department of Cardiology, Qili Hospital of Shandong University, China

ARTICLE INFO

Article history:
Received 19 July 2016
Received in revised form
5 August 2016
Accepted 10 August 2016
Available online 10 August 2016

Keywords:
Exosomes
Microparticles
Hemin

ABSTRACT

Cell-free heme (CFH) and hemoglobin (Hb) have emerged as distinct mediators of acute injury characterized by inflammation and microcirculatory dysfunction in hemolytic conditions and critical illness. Several reports have shown changes in Hb and CFH in specific pathophysiological settings. Using PBS, plasma from patients with sickle cell disease, acute respiratory distress syndrome (ARDS) patients and supernatants from red cells units, we found that commonly used assays and commercially available kits do not distinguish between CFH and Hb. Furthermore, they suffer from a variety of false-positive interferences and limitations (including from bilirubin) that lead to either over- or underestimation of CFH and/or Hb. Moreover, commonly used protocols to separate CFH and Hb based on molecular weight (MWt) are inefficient due to CFH hydrophobicity. In this study, we developed and validated a new approach based on absorbance spectrum deconvolution with least square fitting analyses that overcomes these limitations and simultaneously measures CFH and Hb in simple aqueous buffers, plasma or when associated with red cell derived microvesicles. We show how incorporating other plasma factors that absorb light over the visible wavelength range (specifically bilirubin), coupled with truncating the wavelength range analyzed, or addition of mild detergent significantly improves fits allowing measurement of oxyHb, CFH and metHb with $>90\%$ accuracy. When this approach was applied to samples from SCD patients, we observed that CFH levels are higher than previously reported and of similar magnitude to Hb.

1. Introduction

Cell free heme (plasma free heme+plasma protein bound heme) (CFH) and cell free hemoglobin (Hb), are mediators of tissue injury in hemolytic diseases (e.g. sickle cell disease (SCD), transfusion toxicity, cardiopulmonary bypass, dialysis, infection [1–14]) as well as other diseases not typically associated with hemolysis including environmental poisons and sepsis [15–21]. Cell-free Hb is a potent scavenger of nitric oxide (NO), activates inflammation and undergoes redox cycling reactions that cause oxidative stress [1,8,22–25]. Cell-free heme also stimulates oxidative stress, activates TLR4, and the inflammasome leading to exacerbated inflammation-mediated tissue injury [7,9,19,26–29]. Thus, CFH and Hb elicit tissue injury by overlapping and distinct mechanisms.

Because of the implication that CFH and Hb levels may have on disease mechanisms and therapeutics, it is imperative that methods used to measure each are accurate, sensitive and reproducible. In vivo, CFH and Hb will co-exist and need to be distinguished

* Correspondence to: Department of Pathology, University of Alabama at Birmingham, BMR-2, Room 532, 901 19th Street South, Birmingham, AL 35294, United States.
E-mail address: rakeshpatel@uabmc.edu (R.P. Patel).
[1] These authors contributed equally to the work.

http://dx.doi.org/10.1016/j.redox.2016.08.003

from each other when quantifying. Several methods have been used to measure CFH and Hb in biological matrices. However, these typically rely on a colorimetric detection of CFH and Hb under conditions that may cause Hb denaturation and heme release. Therefore they are unlikely to distinguish between CFH and Hb. Other approaches that improve sensitivity utilize the pseudoperoxidase activity of heme, and link heme to a reporter molecule whose oxidation can be detected by a change in absorbance or fluorescence. Again, these approaches would not distinguish between CFH and Hb, as both are redox active. Our assessment of the literature is that these considerations are often overlooked when measuring CFH and Hb. When appreciated, separation methods based on differing size of CFH and Hb are employed (e.g. Centricon filtration devices). However, these are typically not optimized for separation of hydrophobic compounds such as CFH.

To our knowledge, no systematic study comparing different CFH and Hb measurement protocols have been reported. In this study, we demonstrate that commonly used methods to measure CFH and Hb do not distinguish between them, presenting a problem when both are present in the same medium. We develop a method based on spectral deconvolution, allowing for simultaneous and rapid measurement of CFH and Hb in simple aqueous systems and plasma. *Pros* and *cons* are discussed and applicability to evaluate CFH and Hb in clinical samples demonstrated.

2. Materials and methods

2.1. Materials

All chemicals, reagents and assay kits were purchased from Sigma unless otherwise noted.

2.2. Plasma preparation

Blood was collected by venipuncture from healthy volunteers per UAB IRB approved protocols, and centrifuged $1500 \times g$, 4 °C, 10 min to pellet red blood cells (RBCs). Plasma was collected, stored on ice and used within 24 h.

2.3. Trauma-hemorrhage patient's sample collection

Blood was collected from 37 resuscitated trauma patients according to UAB IRB approved protocols. Blood was centrifuged within 60 min of collection and plasma stored at 4 °C for up to 72 h before freezing in liquid nitrogen. Samples were stored at −80 °C and subsequently thawed on ice for spectral measurements.

2.4. Critically ill patients' sample collection

Plasma was collected from patients with ARDS secondary to Gram negative sepsis and from other critical non-pulmonary conditions, who were intubated and mechanically ventilated in the medical intensive care unit at UAB. All human studies were approved by the UAB Institutional Review Board.

2.5. Sickle cell disease (SCD) patient's sample collection

Within 24 h of admission, blood was collected from SCD patients per UAB IRB approved protocols and recollected every 24 h until discharge or until logistical constraints prevented collection. In order to be included, patients had to have homozygous Hb SS or Hb S Beta Thalassemia (Hb SB0), be 1–21 years old, and admitted for acute chest syndrome (ACS) or vaso-occlusive pain crisis (VOC). Control samples were collected from age-matched African American patients without SCD. Blood was collected in sodium citrate tubes, immediately placed on ice and centrifuged at 1500 rpm, 4 °C for 15 min, within 30 min of collection. Plasma was aliquoted and stored at 4 °C until the aliquots could be rapidly frozen using liquid nitrogen.

2.6. Stored RBC sampling and microvesicle preparation

Leukoreduced RBCs (from six distinct blood donors, with 2 bags collected from one donor) in Adsol were sampled from bags stored for 30–52d in the UAB Blood Bank. Bags were allocated for disposal or expired. RBC were centrifuged $3000 \times g$, 10 min, 4 °C to pellet RBC and provide supernatants. The latter were further processed to isolate microparticles (MP) and exosomes (Exo) by two centrifugations at $10{,}000 \times g$, 30 min, 4 °C (spin 2 and 3) followed by a $150{,}000 \times g$, 2 h, 4 °C (spin 4) centrifugation. Pellets from spins 2 and 3 were combined to give MPs, and pellet from spin 4 contained exosomes. Microvesicle size and number were determined using an NS300 Nanosight (Malvern, UK) with an attached syringe sample pump and 405 nm laser.

2.7. Hemoglobin preparation

Cell-free oxyHb was purified from RBCs and catalase removed as described [30,31]. All hemoglobin was stored in the carbonmonoxide ligated form, and converted to oxyHb or metHb immediately prior to use as described [32]. For cyanide treatment, potassium cyanide (500 mM in 0.1 M KOH) was added to Hb or CFH resulting in cyanide: heme ratios >10; and pH was monitored to keep at 7.4. Final concentration of cyanide is indicated in text.

2.8. Cell-free heme (CFH) preparation

10 mM hemin (Frontier Scientific, UT) was prepared in 0.1 M NaOH, then diluted to 100 μM in PBS, pH 7.4 at 22 °C, fresh on the day of each experiment.

2.9. Conjugated and unconjugated bilirubin

Conjugated (Di-taurine conjugated) bilirubin and unconjugated bilirubin (Lee BioSolutions, MO) were prepared in PBS (2 mg/mL) and ethanol (1 mg/mL) respectively and diluted to indicated concentrations.

2.10. Quantifying CFH, OxyHb, MetHb, and CN-Hb

All CFH and Hb levels are reported in heme (i.e. 1 μM Hb tetramer will be 4 μM Heme expressed per Hb). Various protocols were used to quantify CFH and Hb including:

i) QuantiChrom™ Heme Assay Kit and QuantiChrom™ Hemoglobin Assay Kit (BioAssay, Hayward, CA). CFH and Hb levels were determined using manufacturer's protocols and calibration standards provided. Changes in absorbance at 405 nm were measured using a 96-well plate reader (Victor^3, Perkin Elmer, MA).
ii) CFH or Hb were measured using the TMB Substrate Reagent Set (BD Biosciences, San Jose, CA) with modifications to the manufacturer's protocol: 50 μL PBS or 50 μL diluted plasma (10–200x in PBS) were spiked with oxyHb or CFH to final concentrations of 0–2 μM. PBS or diluted plasma were then mixed with 150 μL of a solution containing hydrogen peroxide and TMB (prepared per manufacturer's instructions), all pre-equilibrated at 37 °C prior to mixing. TMB-oxidation was monitored continuously by following absorbance change at

600 nm (without addition of acid) in a 96-well plate reader over 10 min at 37 °C. Initial rates were acquired and standard curves constructed accordingly.

iii) Modified Drabkins assay: OxyHb was oxidized to metHb using potassium ferricyanide (400 μM final, 10 min at 22 °C), and then to cyanometHb by adding potassium cyanide (500 μM final, 10 min at 22 °C). Change in absorbance at 540 nm *pre-* and *post-* potassium cyanide was measured to determine Hb concentration.

iv) ELISA: Hemoglobin levels were determined by sandwich ELISA (Abcam, ab157707, MA) according to the manufacturer's instructions. Hb levels measured by ELISA were converted and expressed as heme equivalents.

2.11. Cell-free heme (CFH) and hemoglobin (Hb) separation

Two approaches were tested. A) Centricon using Amicon® Ultra Centrifugal Filters (Merck Millipore Ltd, MA), with a 3 kDa MWt cut-off: 100 μL of PBS or plasma containing CFH alone, Hb alone or a mixture of both were added to Centricons and centrifuged at 14,000 × *g*, 4 °C, 2 h. B) Desalting via Micro Bio-Spin™ size-exclusion columns (Bio-Rad, CA), 6 kDa exclusion limit. 100 μL of PBS or plasma with oxyHb and CFH were added to columns and centrifuged at 1500 × *g*, 22 °C for 2 min. Total heme level was determined on *pre-* and *post-* Centricon or *pre-* and *post-* size-exclusion columns to calculate the CFH by QuantiChrom™ Heme assay kit.

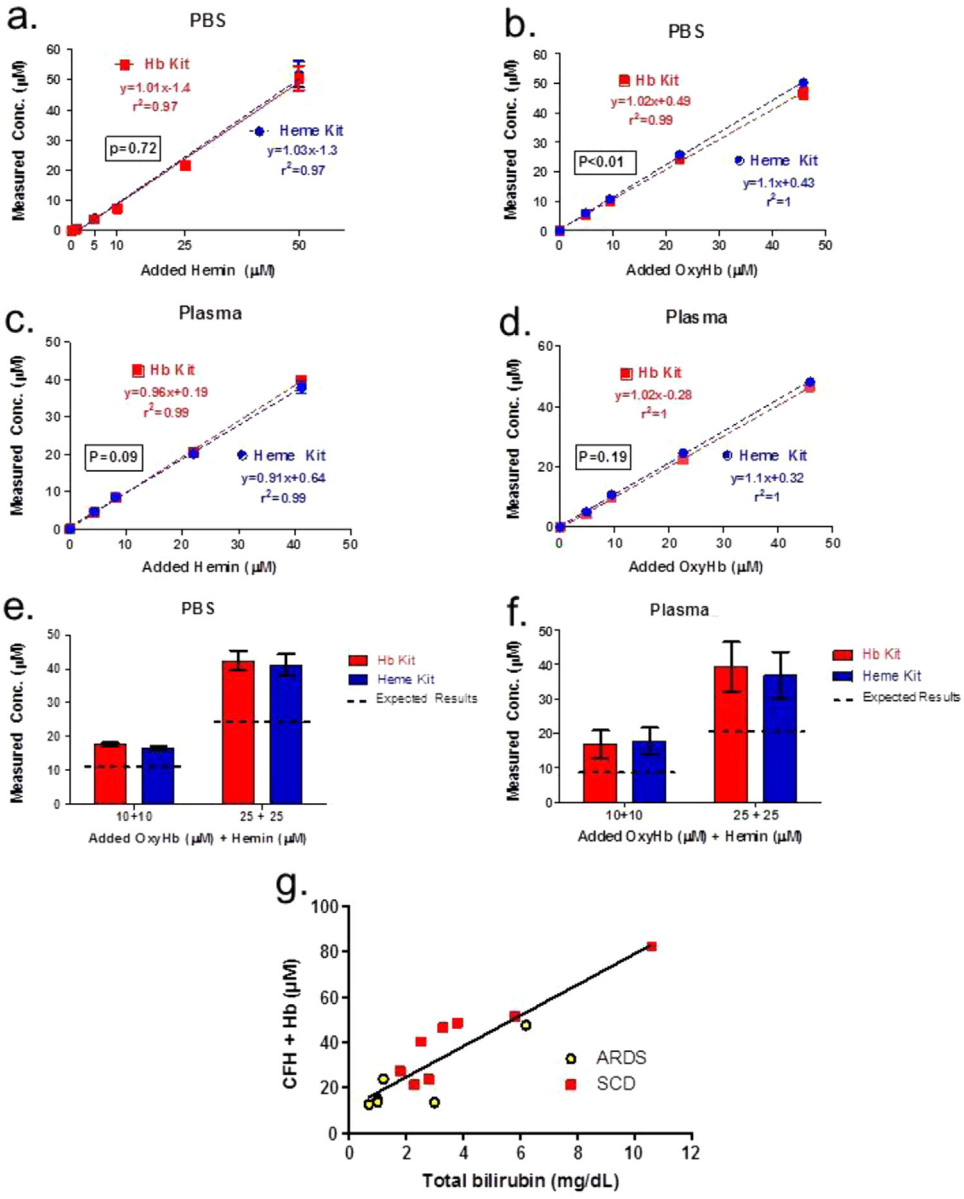

Fig. 1. Cell-free heme (CFH) or hemoglobin (Hb) were dissolved at the indicated concentrations in either PBS or plasma and then measured using the QuantiChrom™ Assay kit for CFH (hemin kit) and Hb (Hb kit), and signal measured and quantified using manufacturer provided standards. **Panel A** shows CFH alone in PBS, **Panel B** oxyHb alone in PBS; **Panel C** plasma spiked with CFH and **Panel D** plasma spiked with oxyHb. Data are mean ± SEM, (n = 3, each replicate from a distinct PBS or plasma (donor) preparation and show values after background subtraction. Best-fit lines were determined by linear regression. Indicated *p*-values show differences between lines. **Panel E–F** show measured concentrations from mixtures of CFH and oxyHb in PBS or plasma respectively. Dashed line indicates expected values if kits were specific for CFH or oxyHb. **Panel G**: Plasma was collected from pediatric SCD patients or ARDS patients and CFH and Hb measured using the QuantiChrom™ assay and plotted against the total bilirubin levels. Each symbol represents a distinct patient sample. Only data with clinical measures of bilirubin were performed as standard of care are shown. Data were analyzed by linear regression ($y = 6.8x - 1.6$, $p < 0.05$ for deviation from zero).

2.12. Albumin depletion

Albumin was removed from plasma using the Pierce™ Albumin Depletion Kit (Thermo Scientific, NY) according to the manufacturer's instructions and confirmed by SDS-PAGE stained with Coomassie Brilliant blue R-250 followed by densitometry.

2.13. Plasma haptoglobin and hemopexin

Plasma haptoglobin and hemopexin were determined by ELISA sandwich assay (Abcam, ab108858 and ab171576 respectively, MA) according to the manufacturer's instructions.

2.14. Spectral deconvolution

Standards for oxyHb, metHb, CFH, conjugated and unconjugated bilirubin and their respective cyano-derivatives were prepared in PBS at pH 7.4 and absorbance between 450 and 700 nm measured by a Beckman UV-visible Spectrophotometer at 1 nm intervals, using 1 cm or 1 mm path length cuvettes at room temperature. Spectra were analyzed by deconvolution algorithms with multilinear regression fitting (Excel) as described [6,33,34].

2.15. Statistical analysis

All results are reported as the mean ± SEM with significant differences considered as those with $p < 0.05$ using tests described in figure legends and calculated using GraphPad Prism 5.

3. Results

3.1. Comparison of CFH and Hb assay kits

3.1.1. Sample alkalinization

CFH or oxyHb alone, or in combination (0–50 μM) were prepared in PBS or plasma and then measured by the QuantiChrom™ Heme or Hemoglobin Assay Kits; both utilize changes in heme absorbance at 405 nm, at alkaline pH. Fig. 1A–D shows that both kits detect CFH and oxyHb, with no differences in the sensitivity for either CFH or oxyHb, except for a very modest, but significant difference with oxyHb in PBS. Furthermore, when mixtures of CFH and oxyHb were tested, each kit measured the sum of the added components (Fig. 1E–F). A further limitation using this approach is that sample displaying significant absorbance in the visible range will lead to false positives. In plasma, this is likely the case where bilirubin is present [35]. Indeed, di-taurine conjugated or unconjugated bilirubin alone gave false positive signals in the QuantiChrom™ Heme and Hemoglobin assay (not shown). Further supporting this is positive correlation between total bilirubin levels and CFH + Hb signal in SCD and ARDS patient plasma (Fig. 1G).

3.1.2. Redox cycling

Another commonly used method utilizes H_2O_2-dependent heme-redox cycling. Fig. 2 shows that the TMB assay measures both CFH and Hb in a dose-dependent manner, but with different sensitivities. For these measurements, TMB oxidation was followed continuously at 600 nm to avoid false positive signals from bilirubin. Fig. 2A shows that in PBS, Hb is more sensitive than CFH whereas in plasma, the relative sensitivity was dependent on the dilution employed (Fig. 2B). Fig. 2C shows the overall slope for TMB oxidation (i.e. Hb + hemin) has little dependence on dilution between 5 and 100 times. In other words, the TMB-dependent signal for plasma does not change, but the relative contribution to

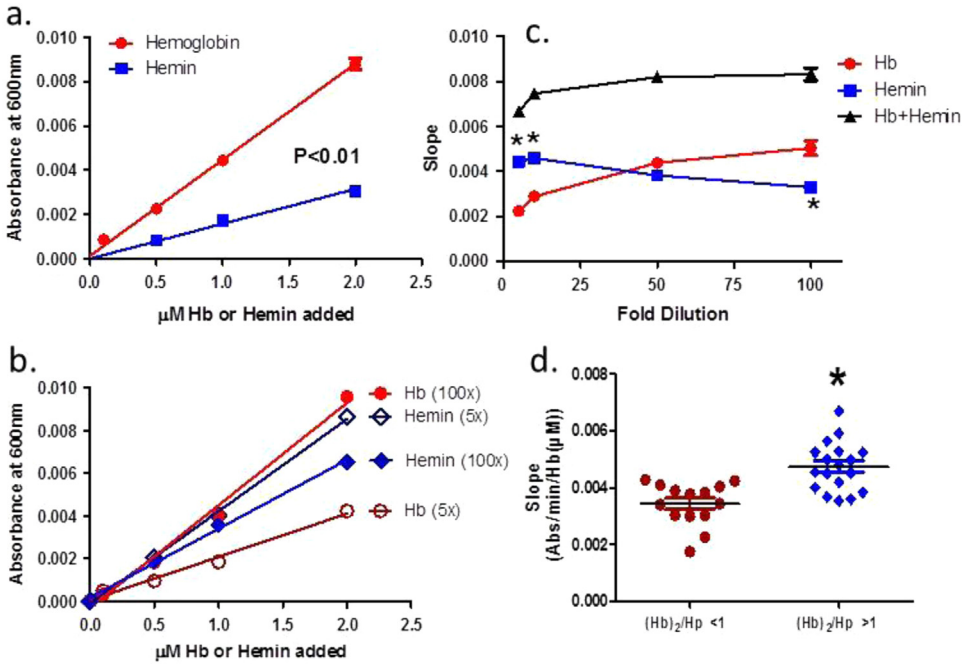

Fig. 2. Cell-free heme (CFH) or hemoglobin (Hb) was dissolved at the indicated concentrations in either PBS **(Panel A)** or plasma (**Panel B–C**) and TMB oxidation at 600 nm measured. For **Panel B**, representative data for 1 plasma preparation are shown after two different dilutions into the TMB assay. For 5X diluted plasma, CFH was more sensitive than Hb, but in 100X diluted plasma, Hb was more sensitive. **Panel C**: Standard curves for Hb and CFH (0–2 μM) dependent TMB oxidation were measured in plasma from 3 distinct donors. Data shows the slope for standard curves and are mean ± SEM, (n = 3). Best-fit lines were determined by linear regression. Indicated P-values show differences between lines. $^*p < 0.01$ by 2-way ANOVA with repeated measures. **Panel D**: the sensitivity of the TMB assay was measured by determining the slope of the Hb standard curve in transfused Trauma patient plasma where the ratio of Hb (in dimer; 1 Hp binds 1 Hb dimer) remained either > 1 or < 1 relative to Hp. $^*p < 0.05$ between groups by *t*-test.

the signal by Hb and CFH will change depending on sample dilution. Plasma donor to donor variability was also noted in this assay (not shown). We speculate this reflects the complex mixture of compounds in plasma (e.g. ascorbate, urate, α-tocopherol, peroxides, hemopexin, haptoglobin) that may increase and/or decrease redox cycling kinetics. To illustrate this, we measured TMB oxidation in plasma collected from resuscitated Trauma patients which was spiked with different amounts of oxyHb to produce samples where the concentration of Hb (in dimer) remained either above or below the haptoglobin (Hp) concentration. When >1 (excess Hb), TMB oxidation was ~two-fold higher (Fig. 2d), indicating that a variable in the TMB assay is not only the amount of Hb, but the relative ratio of Hp to Hb. A further consideration is that inhibitory effect of haptoglobin on Hb redox cycling will depend on the haptoglobin genotype [1].

3.2. Cell-free heme (CFH) and hemoglobin separation

Previous studies have separated CFH and Hb first to delineate the role of protein free *vs.* protein bound heme [7]. To test this, solutions of CFH in PBS or plasma were filtered through 3 kDa cut-off Centricons (Fig. 3A). Fig. 3B–C shows that CFH levels decreased after filtration. Visual observation indicated brown coloration on the membrane suggesting CFH adsorption likely due to hydrophobicity of CFH (not shown). This is further reflected when mixtures of CFH and Hb were processed; Fig. 3D shows that CFH was undetectable in the filtrate, which would lead to CFH underestimation and Hb overestimation. Furthermore, Fig. 3E show total heme levels in SCD plasma after MWt fractionation using 3 kDa Centricons; consistent with Fig. 3A–D, filtration decreased total heme levels to ~1 μM in all cases underscoring that this approach does not separate CFH from Hb.

Next, we tested if a size-exclusion column would allow for sufficient separation of CFH from Hb (Fig. 3F). Fig. 3G shows that with PBS, size-exclusion effectively removes CFH. However, in plasma this was not observed (Fig. 3H). Measured concentrations were the same before and after size-exclusion. This is likely due to hydrophobic interactions between CFH and high MWt proteins indicated by albumin [36] preventing separation of CFH from Hb in PBS (Fig. 3H). However, CFH added into albumin depleted plasma was still not separated by size-exclusion (Fig. 3H) suggesting that multiple proteins might bind CFH and prevent its separation based on MWt.

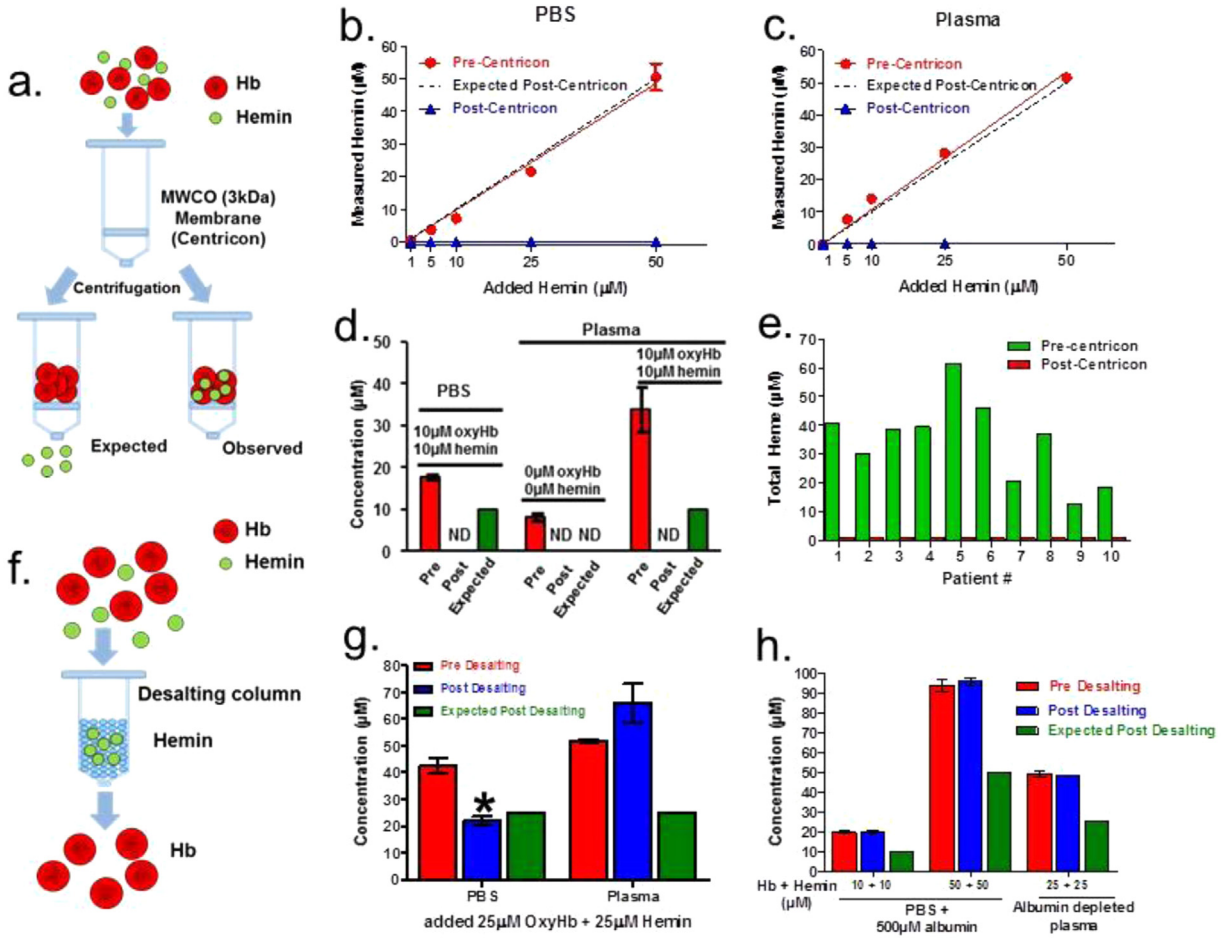

Fig. 3. Panel A: Scheme showing basis of CFH and Hb separation based on MWt filtration. CFH (0–50 μM) dissolved in PBS (**Panel B**) or plasma (**Panel C**) was measured *pre*- and *post*- centricon (3 kDa cut-off) by QuantiChrom™ Heme assay kit. *Pre*-Centricon concentrations of hemin in PBS (B) and plasma (C) are represented by the red line, while the blue line represents measurements of the *post*-Centricon filtrate, and the dotted black line represents the measurements expected post-Centricon. **Panel D** show measured and expected concentrations *pre*- and *post*- centricon separation of mixtures of CFH and oxyHb in PBS and plasma. *Pre*-centricon levels reflect baseline total heme levels in plasma **Panel E**: Plasma was collected from pediatric SCD patients and total heme measured using the QuantiChrom™ assay before and after sample filtration using 3 kDa cut-off Centricon filters (red bars). **Panel F**: Scheme showing basis of CFH and Hb separation using a size-exclusion column. **Panel G**: CFH alone, oxyHb alone, or the combination were dissolved in PBS or plasma and passed through a size-exclusion column and *pre*- and *post*-column levels of Hb and CFH measured using the QuantiChrom™ Heme kit. **Panel H**: Hb and CFH were dissolved in PBS containing 500 μM albumin or albumin depleted human plasma, and processed as described in **Panel G.** Data shown are mean+SEM (n=3). $^{*}p<0.05$ by paired *t*-test relative to pre-desalting. ND=not detectable. (For interpretation of the references to color in this figure legend, the reader is referred to the web version of this article).

3.3. Sample processing

Since sample collection and processing can affect Hb stability which in turn will change the distribution between Hb and CFH, without changing total levels, we tested various collection/storage protocols. Plasma from healthy donors with low bilirubin was used and recovery of added oxyHb or CFH determined. To selectively measure Hb, the Drabkins assay was adapted to account for basal plasma absorbance. Fig. 4A shows representative spectra of oxyHb, metHb and cyanometHb in plasma. The absorbance change at 540 nm, between cyanometHb and metHb was used to determine Hb concentration; delta extinction coefficient calculated to be 4.3 $mM^{-1} \cdot cm^{-1}$ and confirmed in PBS (Fig. 4B). Fig. 4C shows that ferricyanide/cyanide had no effect on CFH absorbance indicating selectivity for Hb. Fig. 4D–E show that both Hb and CFH are fully recoverable in samples stored at 4 °C or −80 °C with rapid (liquid N_2) freezing first. Significant loss of both occurs when stored at 4 °C or placed at −80 °C without first being flash frozen. Also, flash freezing did not alter the disposition between Hb and CFH (not shown). In summary, these data show that plasma samples need to be rapidly frozen to maintain Hb and CFH integrity and levels.

In summary, Figs. 1–4 show that widely used assays for CFH and Hb are not specific for each species, and that depending on plasma intrinsic factors, how MWt based separation was performed, how samples are collected and stored, the levels of CFH may be under- or overestimated.

3.4. Measurement of Hb and CFH in biological matrices

We developed and tested a spectral deconvolution approach to simultaneously quantify Hb and CFH in plasma. This method relies on the fact that CFH has a distinct absorbance spectrum compared to oxidation and ligated forms of Hb present in vivo. Since any absorbance spectrum containing a mixture of different species reflects the concentration of each species multiplied by the extinction coefficient at any given wavelength, spectra can be analyzed by spectral deconvolution with least squares regression fitting, using standard spectra (Fig. 5A) of each species, to determine the concentrations of individual species. We previously validated this approach with RBC stored in Adsol storage media [6] and showed that oxyHb, metHb and CFH can be quantitated by collecting spectra *pre*- and *post*-reaction with potassium cyanide to convert metHb to cyanometHb. Similar results were observed with PBS (not shown).

We next tested the deconvolution method on plasma. A significant challenge is interference from other absorbing components and scatter due to turbidity. As indicated above, bilirubin absorbs light over the visible spectrum (Fig. 5A). We therefore introduced both unconjugated and conjugated bilirubin into spectral deconvolution algorithms. Plasma was collected from healthy donors and spiked with different combinations of oxyHb, metHb and CFH and spectra collected (450–700 nm, 1 cm pathlength). Fig. 5B shows representative spectra from one plasma preparation. Fig. 5C shows residuals for deconvolution fits, excluding bilirubin in the algorithm, and Fig. 5D plots the percent recovery of oxyHb, metHb and CFH relative to the spiked concentration. Under these deconvolution conditions, oxyHb was under estimated by 40% and whereas the average recovery of metHb and CFH was relatively higher, the error associated with these measurements was substantial. Including bilirubin in the deconvolution improved fits by 11.1 ± 1.0 fold (mean ± SEM, n=28) (Fig. 5E), however the residuals (Fig. 5F) remained high and fits poor. This is underscored by lower % recoveries for added oxyHb, overestimation of metHb, and CFH being undetectable (Fig. 5G). Thus, including bilirubin in spectral deconvolution improves accuracy of fits, but does not improve the ability to discern between oxyHb, metHb or CFH. To minimize the contribution of bilirubin, we next tested if limiting the wavelength scan range to between 520 nm and 700 nm would improve fits and ability to distinguish Hb and CFH. Fig. 5H–I show

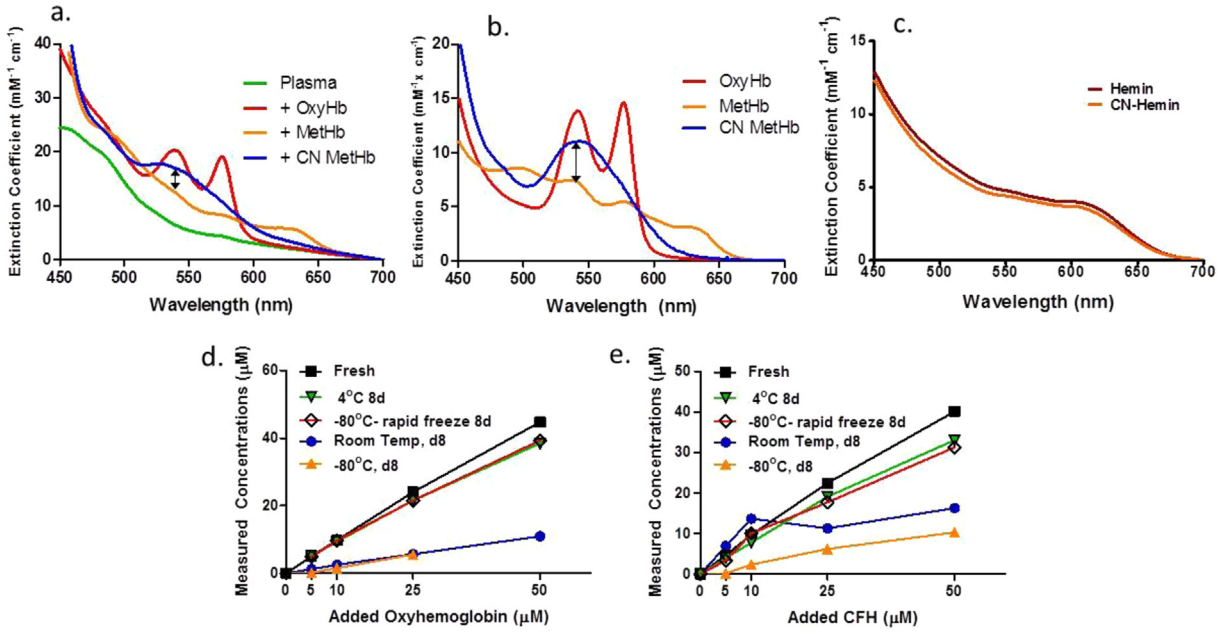

Fig. 4. OxyHb (5 μM) was added to plasma (**Panel A**) or PBS (**Panel B**) and spectra measured. Respective blank spectra were PBS in each case. Potassium ferricyanide (final 400 μM) was then added to convert oxyHb to metHb, and then potassium cyanide (final 500 μM) added to form cyanometHb (pH 7.4). Calculated delta extinction coefficient at 540 nm between metHb and cyanometHb was 4.3 $mM^{-1} \cdot cm^{-1}$ ±0.06 (mean ± SEM, n=3). **Panel C** shows spectra of hemin in the presence or absence of potassium ferricyanide and potassium cyanide. Plasma was collected from healthy volunteers and spiked with indicated concentrations of oxyHb (**Panel D**) or CFH (**Panel E**). OxyHb or CFH was added to plasma and then measured immediately and then stored at room temperature, 4 °C, −80 °C, or first rapidly frozen in liquid N_2 and then stored at −80 °C for 8d. Total heme was measured by QuantiChrom™ Heme assay kit. Hb was measured as outlined in **Panel A**.

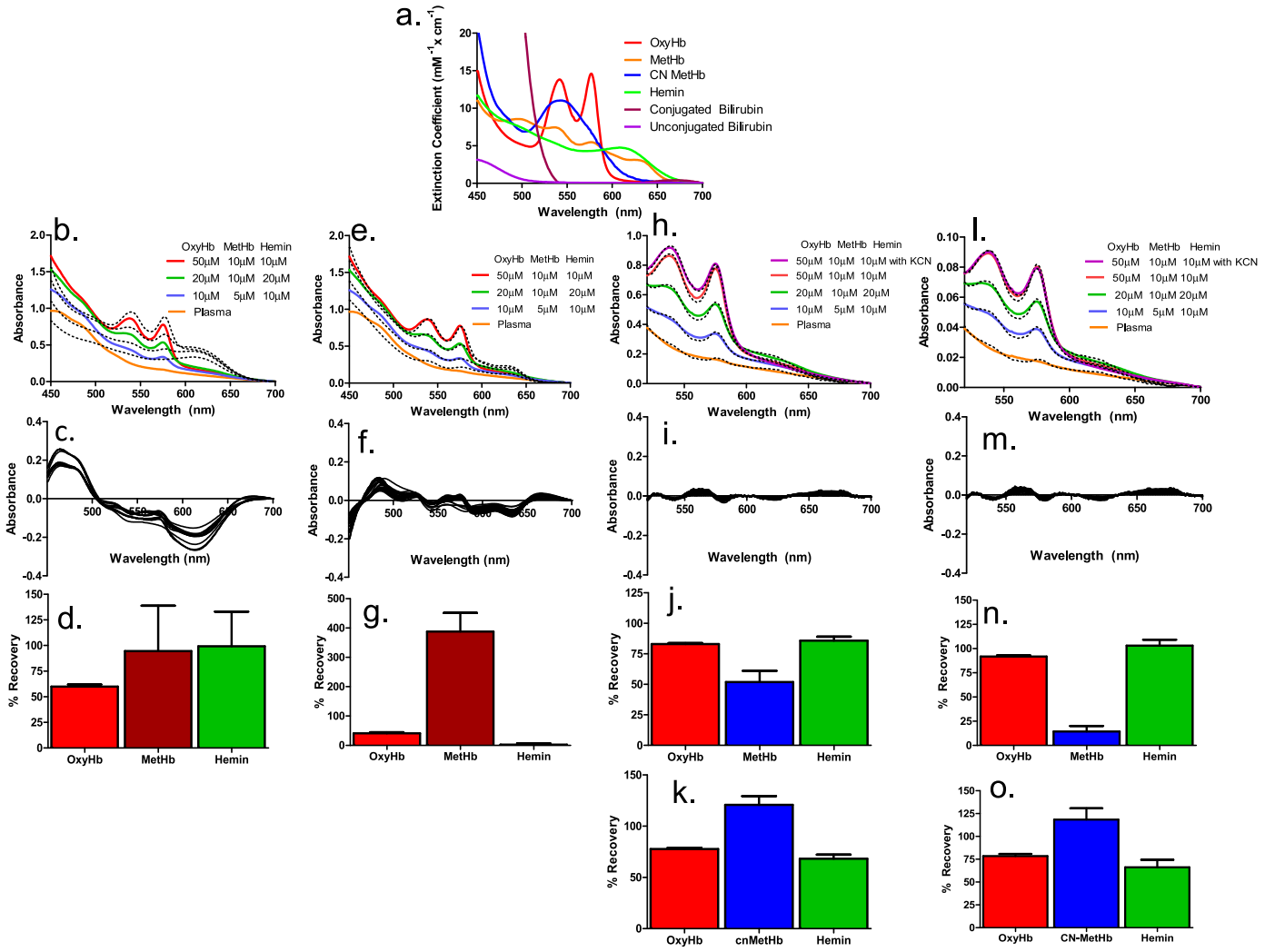

Fig. 5. Panel A: Standard spectra of oxyHb, metHb, cyanometHb, hemin, conjugated and unconjugated bilirubin prepared in PBS, pH 7.4. Plasma was prepared from 3 healthy donors and spiked with indicated concentrations of oxyHb, metHb and CFH. Spectra were measured between 450 and 700 nm in 1 cm or 1 mm cuvettes as indicated. Also where shown, spectra were measured after addition of potassium cyanide (400 μM, 10 min, 22 °C). *Conditions:* **Panels B–D**: 1 cm cuvette, deconvolution using oxyHb, metHb and CFH between 450 and 700 nm; **Panels E–G**: 1 cm cuvette, deconvolution using oxyHb, metHb, CFH, conjugated bilirubin and unconjugated bilirubin between 450 and 700 nm; **Panels H–K**: 1 cm cuvette, deconvolution using oxyHb, metHb, CFH, conjugated bilirubin, unconjugated bilirubin or with cyanometHb between 520 and 700 nm; **Panels I–O**: 1 mm cuvette, deconvolution using oxyHb, metHb, CFH, conjugated bilirubin, unconjugated bilirubin, or with cyanometHb between 520 and 700 nm. **Panels B, E, H and L** show representative spectra from a single donor with dotted lines indicated fits after deconvolution. **Panels C, F, I and M** show residuals for deconvolution fits for respective spectra. **Panels D, G, J, K, N and O** show percent recovery of added oxyHb, metHb, CFH and cyanometHb from respective deconvolution analyses across all groups. Data in bar graphs are mean ± SEM (n=3).

that fits improved by 44.0 ± 5.5 fold (mean ± SEM, n=28). Using these conditions, 83 ± 0.8% of added oxyHb and 86 ± 3.2% of added CFH was measurable (mean ± SEM, n=4); however metHb was underestimated by ~50% (Fig. 5J). To improve metHb detection, we added potassium cyanide to form cyanometHb and then performed deconvolution analysis again. In this case (Fig. 5K) both oxyHb and CFH recovery decreased slightly (78 ± 1.2% and 68 ± 4% respectively), but metHb was now detectable with a recovery of ~110%. Finally, to limit scatter associated with turbidity, we measured spectra from the same sample in a 1 mm pathlength cuvette; while this will decrease sensitivity per the Beer-Lambert law, scatter effects will also diminished. Fig. 5L–N shows that this protocol resulted in the most optimal oxyHb and CFH recovery (92 ± 1.3% and 103 ± 6.1% respectively), but again cyanide was required to detect metHb (Fig. 5O). In summary, these data suggest that deconvolution of visible spectra of plasma ± potassium cyanide, collected between 520 and 700 nm in both 1 cm and 1 mm cuvettes is able to reliably and simultaneously quantitate oxyHb, metHb (via CNmetHb) and CFH with >90% accuracy.

3.4.1. *Application of deconvolution method to SCD plasma*

61 plasma samples were collected from 19 pediatric SCD patients and 7 plasmas from age- and sex-matched control patients (see Table 1). Visible spectra were measured from 450–700 nm in 1 mm cuvettes and deconvolution analyses performed between 520 and 700 nm. Fig. 6A shows representative spectra of SCD plasma that contained varying ratios of oxyHb: CFH. Fig. 6B plots the oxyHb, metHb and CFH levels, and Fig. 6C the relative concentrations of oxyHb, metHb (CNmetHb) and CFH within each sample. Fig. 6D plots the relationship between oxyHb and CFH in VOC and ACS samples. Interestingly, while there was no significant correlation in ACS samples, with VOC, a positive correlation between oxyHb and CFH was observed. Finally, to further validate the deconvolution results, Hb levels were also measured by ELISA. Fig. 6E shows a correlation of 0.94 between the two approaches.

Table 1
Demographic data of the control and sickle cell patients included in this study. A total of 61 plasma samples were collected from 19 pediatric SCD patients. Samples for 2 out of the 19 patients were collected on separate admissions. Two patients were excluded due to improper handling of their samples (a total of 4 plasma samples), 3 samples excluded from analysis as they were collected during wellness visits and 1 sample excluded as it was collected from a patient who underwent red cell apheresis within the previous 24 h prior to collection. Of the 17 included patients, 12 were admitted with vasoocclusive crisis (VOC) and 6 with acute chest syndrome (ACS). Control patients were obtained from a population of otherwise healthy, age and race-matched patients undergoing procedures in the OR. These procedures included 2 patients undergoing a cardiac catheterization, one inguinal hernia repair, one esophageal foreign body removal, one keloid injection, one circumcision, and one umbilical hernia repair. One control sample was excluded from analysis secondary to the presence of chronic health conditions including a past heart transplant which was not known at the time of collection.

		Control	Sickle cell patient		
			All	VOC	ACS
N		7	17	12	5
Mean age (yrs)		8.4 (4–17)	12.3 (4–19)	13.6 (5–19)	9 (4–18)
Gender	Male	5	8	6	2
	Female	2	9	6	3
Race	African American	7	16	11	5
	Hispanic	0	1	1	0
Hb	SS	0	17	12	5
	Sβ0-thalassemia	0	0	9	0
Chronic therapy	Hydroxyurea	0	15	11	4
	Monthly transfusion	0	1	1	0

3.4.2. *Application of deconvolution method to RBC-derived microvesicles*

Recent studies have suggested that red-cell derived microvesicles contain CFH and mediate endothelial dysfunction in SCD [29,37]. To test the deconvolution method and evaluate if microvesicles formed during RBC storage similarly contain CFH, microparticles (MP) and exosomes (Exo) were prepared from stored RBCs. MPs were more abundant ($284 \pm 59 \times 10^9$ vs. $89 \pm 20 \times 10^9$ particles/mL) and larger (136 ± 4.6 nm and 113 ± 9.1 nm) compared to Exo (all data mean ± SEM, n=7). Fig. 7A shows representative spectra of MP and Exo together with fits from deconvolution analyses; residuals are shown in Fig. 7B–C. Fits were relatively poor due to turbidity, but improved between 3 and 16 fold by addition of 0.01–0.05% triton (Fig. 7A–C). Fig. 7D plots the concentration of Hb and CFH normalized per mL of starting material and Fig. 7E per particle. CFH was lower compared to Hb per MP or Exo, with greater number of particles leading to higher Hb amounts between MP and Exo (Fig. 7D).

4. Discussion

The emerging importance of Hb and CFH in acute diseases characterized by oxidative stress and associated with low to high levels of hemolysis is underscored by both biomarker and predictive considerations, where these species are associated with adverse outcomes, and *pre*-clinical data showing causative roles in mediating vascular and end-organ inflammation and toxicity. These considerations necessitate methods that can measure each selectively and with sufficient sensitivity in biological matrices.

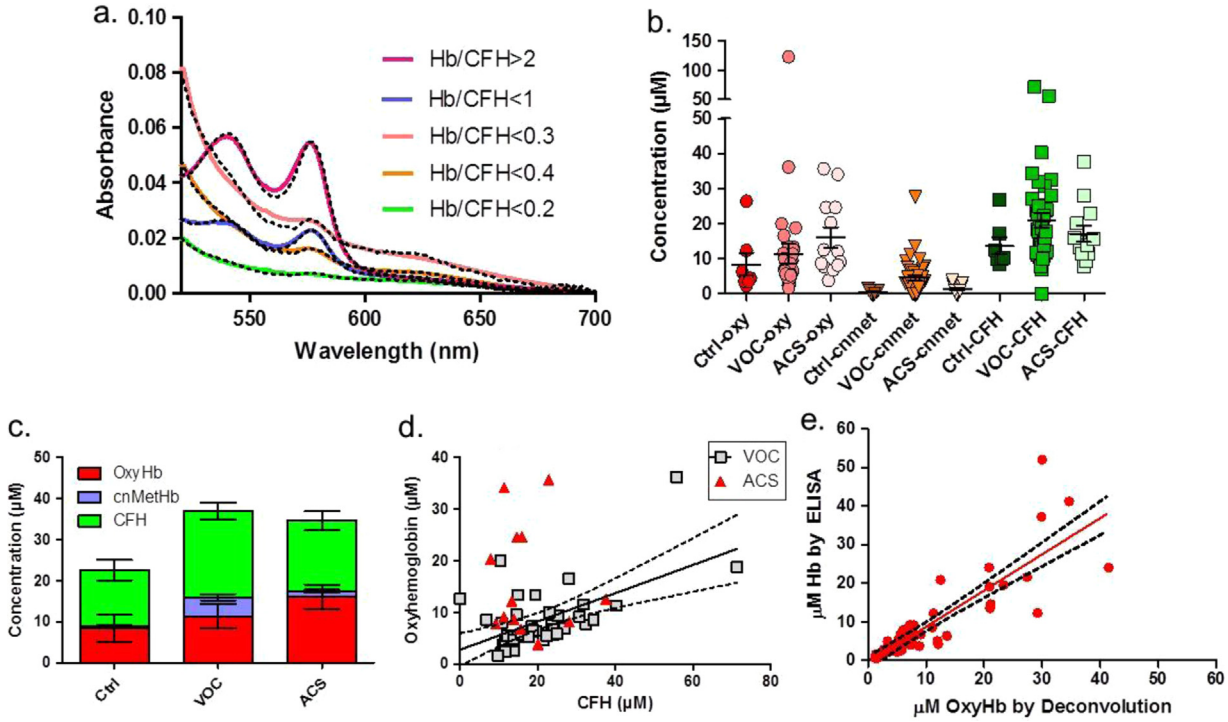

Fig. 6. Plasma was collected from control or SCD patients and spectra measured *pre*- and *post*- potassium cyanide treatment in 1 mm cuvettes. Spectra were deconvoluted between 520 and 700 nm using base spectra of oxyHb, metHb, CNmetHb (when CN was added), hemin, conjugated bilirubin and unconjugated bilirubin. **Panel A**: representative spectra of SCD plasma samples in which varying ratios of Hb:CFH were determined. Dotted lines represent fits from deconvolution. **Panel B**: Concentration of oxyHb, metHb (derived from CN-metHb after potassium cyanide addition) and CFH measured in control or SCD patients with VOC or ACS. **Panel C**: Distribution of oxyHb, metHb and CFH in control, or SCD patients with VOC or ACS. **Panel D**: Relationship between oxyHb and CFH in SCD-VOC and SCD-ACS patients. Shown are best-fit lines determined by linear regression with 95% confidence interval bands for VOC group only (n=40). No significant relationship between oxyHb and CFH in ACS was observed (n=13). **Panel E**: Hemoglobin levels were determined by ELISA and deconvolution. Line shows best fit by linear regression with 95% confident interval.

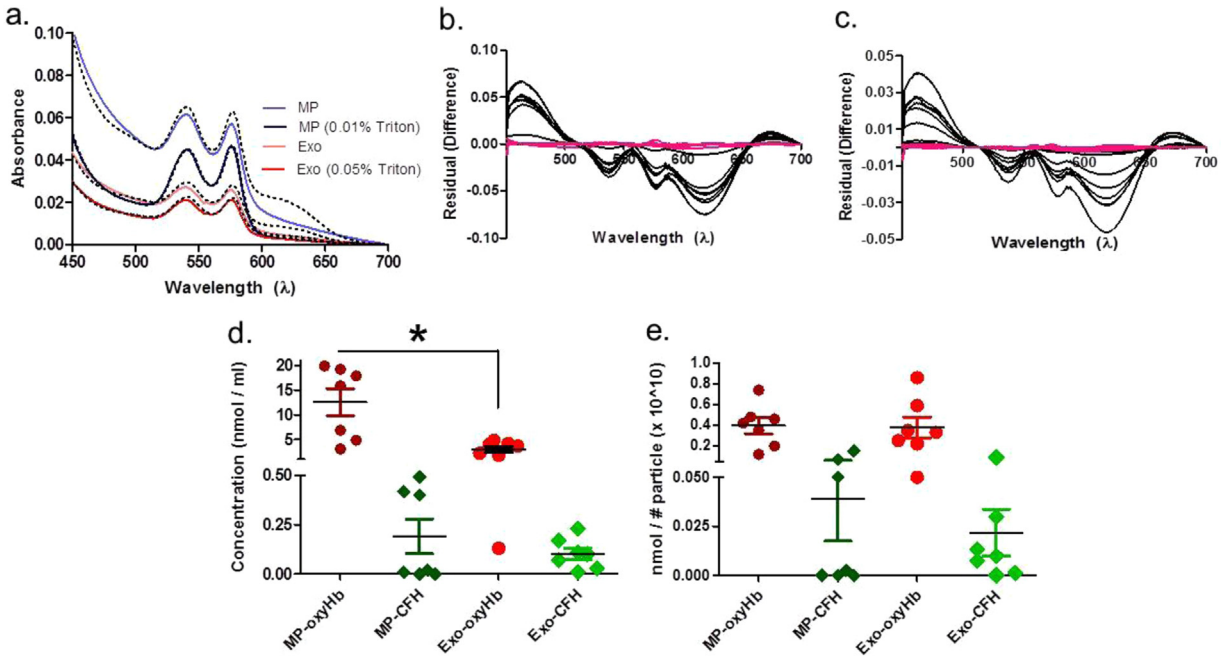

Fig. 7. Microparticles and exosomes were prepared from leukoreduced RBC (in Adsol) collected from bags stored for 30–52d. **Panel A:** Representative absorbance spectra of MP and exosome fractions in the absence or presence of 0.01–0.05% triton. Dotted lines show best fits by spectral deconvolution using base spectra of oxyHb, metHb, and hemin. **Panel B–C** show residuals before (black lines) and after triton (red lines) for microparticles and exosomes respectively. **Panel D** plots concentrations of oxyHb and CFH in microparticle (MP) and exosome fractions (Exo). Panel E plots these species per particle. $^{*}p < 0.05$ by paired *t*-test. Data are mean ± SEM (n=7). (For interpretation of the references to color in this figure legend, the reader is referred to the web version of this article).

Several methods have been employed to measure both Hb and CFH together (i.e. total heme), Hb or CFH alone. As shown herein, most currently used methods are not selective, as they rely on properties that are similar for both CFH and Hb. We have not tested all previously used approaches but note that redox cycling and/or absorbance changes at a single wavelength are commonly used, and other approaches e.g. heme-pyridine extraction, rely on removing CFH from Hb first, again precluding distinguishing between these species. Since these methods will measure both CFH and Hb at least additively, one or the other will be overestimated. This potential error is compounded if sample collection and processing leads to change in disposition between different heme-species (for example metHb is more sensitive to degradation by freeze-thawing and heme sequestered in hydrophobic compartments (e.g. lipids) will be lost if these are pelleted), and by the fact that variables that affect CFH and Hb redox cycling are often overlooked. Moreover, single wavelength monitoring does not account for other species that may absorb at that wavelength.

We applied a spectral deconvolution method to measure Hb and CFH in plasma. Using a stepwise process that improved spectral fits by least squares fitting, we show that inclusion of bilirubin spectra, limiting the wavelength range over which deconvolution is performed and using a 1 mm cuvette, allowed measurement of Hb and CFH with $>90\%$ accuracy, and in plasmas from different donors that displayed distinct degrees of turbidity. Addition of cyanide, to form cyanometHb then allows for metHb measurement. There are limitations to this approach however. It is possible that we have not accounted for all absorbing species in plasma. Absorbance based approaches may be limited in terms of sensitivity, however spiking with 2 μM of heme-species was readily detectable. Another consideration is if one heme-species is present at much higher concentrations than the other, sensitivity of deconvolution to discern low levels will be challenging. Indeed, the largest discrepancy between deconvolution results with ELISA based measures of oxyHb was in plasma that had the highest levels of oxyHb (>100 μM, not shown). This limitation is addressable by sample dilution however. Finally, absorbance will measure both free and bound (to haptoglobin and hemopexin) forms of Hb and CFH. This can be viewed as both an advantage and possible limitation as it allows measurement of the total, but the free forms are likely more important for mediating toxicity. Irrespective of the method employed, it is important to measure these acute phase proteins at the same time as Hb and CFH, to fully evaluate the role of the latter in a given pathophysiological setting. We also note that there are other methods selective for Hb or CFH. Immuno-based (antibody capture ELISA or Western blotting) are selective for Hb but will not measure CFH. CFH can be selectively measured by addition of ApoMb and following Mb formation [38] and a recent study reports on fluorescent heme-sensors for cell-based measurements [39]. However, the amenability of such approaches to plasma remains unclear.

We also applied deconvolution to quantify Hb and CFH in MP and Exo isolated from stored RBCs. The concept that hemoglobin and heme may be carried in red cell derived vesicles is relatively new [8,29]. No studies to our knowledge have applied vigorous protocols to measure the exact and relative amounts of hemoglobin and heme in these, however. The main limitation of sample turbidity and light scattering was overcome by addition of mild detergent. Using this approach we showed that per particle, Hb and CFH does not differ between MP or Exo, with Hb being 10–15 fold greater than CFH. Notably, while a normal distribution of CFH was observed in Exo, with MP two populations could be discerned with CFH being detectable or not. Further studies are required to test if these are indeed distinct particles.

A clear advantage of the deconvolution approach is its simplicity, most labs have access to UV–visible spectrophotometers and the fact that oxyHb, metHb and CFH can be determined simultaneously with little sample handling and reactions involved. We suggest that spectra be measured preferably on freshly obtained samples, or samples undergone a single freeze-thaw cycle, *pre-* and *post*-cyanide reaction using both 1 cm and 1 mm cuvettes. Using this approach we measured plasma Hb and CFH in pediatric

SCD patients diagnosed with VOC and ACS. The mean and range of concentrations of oxyHb were similar to that observed in adult SCD [9]. Our measures of CFH levels however, were higher than previous reports [27]. We speculate this difference is due to underestimation of CFH in prior studies due to use of Centricons to separate plasma CFH and Hb, which we show (Fig. 3) removes CFH from plasma or PBS. Notably, CFH levels were similar in magnitude to oxyHb. Thus, quantitatively oxyHb may not be the predominant free heme-containing species in hemolytic syndromes. We also note that there was significant variance in Hb and CFH levels amongst VOC and ACS groups. Despite this a positive correlation between HB and CFH was observed in VOC, but not ACS. We have no mechanistic insights into this potential difference between VOC and ACS, and note that sample size limitations preclude forwarding generalizable conclusions and we present these data to underscore the need for more extensive assessment of Hb *vs.* CFH levels in other disease states using accurate methods, which will in turn better complement studies evaluating the causative roles of these species in disease pathogenesis.

Author contributions

JYO, JH, JL, JDK, JFP, AG and RPP conceptualized the study; JYO, JH, XX, KG, MZ, RPP designed and performed the experiments, analyzed the results, and wrote the manuscript; and all authors critically commented on the manuscript.

Disclosure of conflicts of interest

The authors declare no competing financial interests.

Acknowledgments

We acknowledge assistance from Dr Prasanna Palabindela for SCD patient sample collection.

References

[1] D.J. Schaer, P.W. Buehler, A.I. Alayash, J.D. Belcher, G.M. Vercellotti, Hemolysis and free hemoglobin revisited: exploring hemoglobin and hemin scavengers as a novel class of therapeutic proteins, Blood 121 (2013) 1276–1284.
[2] D. Chiabrando, F. Vinchi, V. Fiorito, S. Mercurio, E. Tolosano, Heme in pathophysiology: a matter of scavenging, metabolism and trafficking across cell membranes, Front. Pharmacol. 5 (2014) 61.
[3] F.T. Billings, S.K. Ball, L.J. Roberts 2nd, M. Pretorius, Postoperative acute kidney injury is associated with hemoglobinemia and an enhanced oxidative stress response, Free Radic. Biol. Med. 50 (2011) 1480–1487.
[4] I.C. Vermeulen Windsant, M.G. Snoeijs, S.J. Hanssen, S. Altintas, J.H. Heijmans, T.A. Koeppel, G.W. Schurink, W.A. Buurman, M.J. Jacobs, Hemolysis is associated with acute kidney injury during major aortic surgery, Kidney Int. 77 (2010) 913–920.
[5] C. Meyer, C. Heiss, C. Drexhage, E.S. Kehmeier, J. Balzer, A. Muhlfeld, M. W. Merx, T. Lauer, H. Kuhl, J. Floege, M. Kelm, T. Rassaf, Hemodialysis-induced release of hemoglobin limits nitric oxide bioavailability and impairs vascular function, J. Am. Coll. Cardiol. 55 (2010) 454–459.
[6] R. Stapley, C. Rodriguez, J.Y. Oh, J. Honavar, A. Brandon, B.M. Wagener, M. B. Marques, J.A. Weinberg, J.D. Kerby, J.F. Pittet, R.P. Patel, RBC washing, nitrite therapy, and anti-heme therapies prevent stored RBC toxicity after trauma-hemorrhage, Free Radic. Biol. Med. (2015).
[7] S. Ghosh, O.A. Adisa, P. Chappa, F. Tan, K.A. Jackson, D.R. Archer, S.F. Ofori-Acquah, Extracellular hemin crisis triggers acute chest syndrome in sickle mice, J. Clin. Investig. 123 (2013) 4809–4820.
[8] M.T. Gladwin, D.B. Kim-Shapiro, Storage lesion in banked blood due to hemolysis-dependent disruption of nitric oxide homeostasis, Curr. Opin. Hematol. 16 (2009) 515–523.
[9] C.D. Reiter, X. Wang, J.E. Tanus-Santos, N. Hogg, R.O. Cannon 3rd, A. N. Schechter, M.T. Gladwin, Cell-free hemoglobin limits nitric oxide bioavailability in sickle-cell disease, Nat. Med. 8 (2002) 1383–1389.
[10] A. Pamplona, A. Ferreira, J. Balla, V. Jeney, G. Balla, S. Epiphanio, A. Chora, C. D. Rodrigues, I.P. Gregoire, M. Cunha-Rodrigues, S. Portugal, M.P. Soares, M. M. Mota, Heme oxygenase-1 and carbon monoxide suppress the pathogenesis of experimental cerebral malaria, Nat. Med. 13 (2007) 703–710.
[11] E. Seixas, R. Gozzelino, A. Chora, A. Ferreira, G. Silva, R. Larsen, S. Rebelo, C. Penido, N.R. Smith, A. Coutinho, M.P. Soares, Heme oxygenase-1 affords protection against noncerebral forms of severe malaria, Proc. Natl. Acad. Sci. USA 106 (2009) 15837–15842.
[12] F. Vinchi, L. De Franceschi, A. Ghigo, T. Townes, J. Cimino, L. Silengo, E. Hirsch, F. Altruda, E. Tolosano, Hemopexin therapy improves cardiovascular function by preventing heme-induced endothelial toxicity in mouse models of hemolytic diseases, Circulation 127 (2013) 1317–1329.
[13] J.H. Baek, F. D'Agnillo, F. Vallelian, C.P. Pereira, M.C. Williams, Y. Jia, D.J. Schaer, P.W. Buehler, Hemoglobin-driven pathophysiology is an in vivo consequence of the red blood cell storage lesion that can be attenuated in guinea pigs by haptoglobin therapy, J. Clin. Investig. 122 (2012) 1444–1458.
[14] E.L. Brittain, D.R. Janz, E.D. Austin, J.A. Bastarache, L.A. Wheeler, L.B. Ware, A. R. Hemnes, Elevation of plasma cell free hemoglobin in pulmonary arterial hypertension, Chest (2014).
[15] D.R. Janz, J.A. Bastarache, G. Sills, N. Wickersham, A.K. May, G.R. Bernard, L. B. Ware, Association between haptoglobin, hemopexin and mortality in adults with sepsis, Crit. Care 17 (2013) R272.
[16] M. Adamzik, T. Hamburger, F. Petrat, J. Peters, H. de Groot, M. Hartmann, Free hemoglobin concentration in severe sepsis: methods of measurement and prediction of outcome, Crit. Care 16 (2012) R125.
[17] D.R. Janz, J.A. Bastarache, J.F. Peterson, G. Sills, N. Wickersham, A.K. May, L. J. Roberts 2nd, L.B. Ware, Association between cell-free hemoglobin, acetaminophen, and mortality in patients with sepsis: an observational study, Crit. Care Med. 41 (2013) 784–790.
[18] R. Larsen, R. Gozzelino, V. Jeney, L. Tokaji, F.A. Bozza, A.M. Japiassu, D. Bonaparte, M.M. Cavalcante, A. Chora, A. Ferreira, I. Marguti, S. Cardoso, N. Sepulveda, A. Smith, M.P. Soares, A central role for free heme in the pathogenesis of severe sepsis, Sci. Transl. Med. 2 (2010), 51ra71.
[19] T. Lin, D. Maita, S.R. Thundivalappil, F.E. Riley, J. Hambsch, L.J. Van Marter, H. A. Christou, L. Berra, S. Fagan, D.C. Christiani, H.S. Warren, Hemopexin in severe inflammation and infection: mouse models and human diseases, Crit. Care 19 (2015) 166.
[20] S. Aggarwal, A. Lam, S. Bolisetty, M.A. Carlisle, A. Traylor, A. Agarwal, S. Matalon, Heme attenuation ameliorates irritant gas inhalation-induced acute lung injury, Antioxid. Redox Signal. 24 (2016) 99–112.
[21] C.M. Shaver, C.P. Upchurch, D.R. Janz, B.S. Grove, N. Putz, N. Wickersham, S. I. Dikalov, L.B. Ware, J.A. Bastarache, Cell-free hemoglobin: a novel mediator of acute lung injury, Am. J. Physiol. Lung Cell. Mol. Physiol. (2016), http://dx.doi.org/10.1152/ajplung.00155.2015.
[22] R.P. Patel, Biochemical aspects of the reaction of hemoglobin and NO: implications for Hb-based blood substitutes, Free Radic. Biol. Med. 28 (2000) 1518–1525.
[23] C. Lisk, D. Kominsky, S. Ehrentraut, J. Bonaventura, R. Nuss, K. Hassell, E. Nozik-Grayck, D.C. Irwin, Hemoglobin-induced endothelial cell permeability is controlled, in part, via a myeloid differentiation primary response gene-88-dependent signaling mechanism, Am. J. Respir. Cell Mol. Biol. 49 (2013) 619–626.
[24] C.E. Cooper, D.J. Schaer, P.W. Buehler, M.T. Wilson, B.J. Reeder, G. Silkstone, D. A. Svistunenko, L. Bulow, A.I. Alayash, Haptoglobin binding stabilizes hemoglobin ferryl iron and the globin radical on tyrosine beta145, Antioxid. Redox Signal. 18 (2013) 2264–2273.
[25] A.I. Alayash, R.P. Patel, R.E. Cashon, Redox reactions of hemoglobin and myoglobin: biological and toxicological implications, Antioxid. Redox Signal. 3 (2001) 313–327.
[26] J.D. Belcher, C. Chen, J. Nguyen, L. Milbauer, F. Abdulla, A.I. Alayash, A. Smith, K. A. Nath, R.P. Hebbel, G.M. Vercellotti, Heme triggers TLR4 signaling leading to endothelial cell activation and vaso-occlusion in murine sickle cell disease, Blood 123 (2014) 377–390.
[27] O.A. Adisa, Y. Hu, S. Ghosh, D. Aryee, I. Osunkwo, S.F. Ofori-Acquah, Association between plasma free haem and incidence of vaso-occlusive episodes and acute chest syndrome in children with sickle cell disease, Br. J. Haematol. 162 (2013) 702–705.
[28] T. Lin, F. Sammy, H. Yang, S. Thundivalappil, J. Hellman, K.J. Tracey, H. S. Warren, Identification of hemopexin as an anti-inflammatory factor that inhibits synergy of hemoglobin with HMGB1 in sterile and infectious inflammation, J. Immunol. 189 (2012) 2017–2022.
[29] S.M. Camus, J.A. De Moraes, P. Bonnin, P. Abbyad, S. Le Jeune, F. Lionnet, L. Loufrani, L. Grimaud, J.C. Lambry, D. Charue, L. Kiger, J.M. Renard, C. Larroque, H. Le Clesiau, A. Tedgui, P. Bruneval, C. Barja-Fidalgo, A. Alexandrou, P.L. Tharaux, C.M. Boulanger, O.P. Blanc-Brude, Circulating cell membrane microparticles transfer heme to endothelial cells and trigger vasoocclusions in sickle cell disease, Blood 125 (2015) 3805–3814.
[30] R. Stapley, B.Y. Owusu, A. Brandon, M. Cusick, C. Rodriguez, M.B. Marques, J. D. Kerby, S.R. Barnum, J.A. Weinberg, J.R. Lancaster Jr, R.P. Patel, Erythrocyte storage increases rates of NO and nitrite scavenging: implications for transfusion-related toxicity, Biochem. J. 446 (2012) 499–508.
[31] R.P. Patel, D.A. Svistunenko, V.M. Darley-Usmar, M.C. Symons, M.T. Wilson, Redox cycling of human methaemoglobin by H_2O_2 yields persistent ferryl iron and protein based radicals, Free Radic. Res. 25 (1996) 117–123.
[32] T.S. Isbell, M.T. Gladwin, R.P. Patel, Hemoglobin oxygen fractional saturation regulates nitrite-dependent vasodilation of aortic ring bioassays, Am. J. Physiol. Heart Circ. Physiol. 293 (2007) H2565–H2572.
[33] S. Basu, R. Grubina, J. Huang, J. Conradie, Z. Huang, A. Jeffers, A. Jiang, X. He,

I. Azarov, R. Seibert, A. Mehta, R. Patel, S.B. King, N. Hogg, A. Ghosh, M. T. Gladwin, D.B. Kim-Shapiro, Catalytic generation of N_2O_3 by the concerted nitrite reductase and anhydrase activity of hemoglobin, Nat. Chem. Biol. 3 (2007) 785–794.

[34] Z. Huang, S. Shiva, D.B. Kim-Shapiro, R.P. Patel, L.A. Ringwood, C.E. Irby, K. T. Huang, C. Ho, N. Hogg, A.N. Schechter, M.T. Gladwin, Enzymatic function of hemoglobin as a nitrite reductase that produces NO under allosteric control, J. Clin. Investig. 115 (2005) 2099–2107.

[35] V.F. Fairbanks, S.C. Ziesmer, P.C. O'Brien, Methods for measuring plasma hemoglobin in micromolar concentration compared, Clin. Chem. 38 (1992) 132–140.

[36] P. Ascenzi, A. di Masi, G. Fanali, M. Fasano, Heme-albumin: an honorary enzyme, Cell Death Dis. 6 (2015) e1895.

[37] S.M. Camus, B. Gausseres, P. Bonnin, L. Loufrani, L. Grimaud, D. Charue, J.A. De Moraes, J.M. Renard, A. Tedgui, C.M. Boulanger, P.L. Tharaux, O.P. Blanc-Brude, Erythrocyte microparticles can induce kidney vaso-occlusions in a murine model of sickle cell disease, Blood 120 (2012) 5050–5058.

[38] M.S. Hargrove, T. Whitaker, J.S. Olson, R.J. Vali, A.J. Mathews, Quaternary structure regulates hemin dissociation from human hemoglobin, J. Biol. Chem. 272 (1997) 17385–17389.

[39] D.A. Hanna, R.M. Harvey, O. Martinez-Guzman, X. Yuan, B. Chandrasekharan, G. Raju, F.W. Outten, I. Hamza, A.R. Reddi, Heme dynamics and trafficking factors revealed by genetically encoded fluorescent heme sensors, Proc. Natl. Acad. Sci. USA (2016).